2. IRON-CONTAINING SUPERCONDUCTORS FROM THE VIEWPOINT OF CHEMISTS: THERMODYNAMIC STABILITY AND SUBSTITUTION LIMITS IN $La_{1-x}Ln_xFeAsO_{1-y}$ HIGH-TEMPERATURE SUPERCONDUCTORS (Ln = Ce–Er and Y)

E. Get'man[1], Yu. Oleksii[1,2], O. Mariichak[1], L. Ardanova[3], S. Radio[1]

Abstract

Within the framework of V. S. Urusov's crystal energy approach, we calculated mixing energies (interaction parameters), critical decomposition (stability) temperatures and built the domes of the decomposition of solid solutions of the following systems: $La_{1-x}Ce_xFeAsO_{0.65}$, $La_{1-x}Pr_xFeAsO_{0.65}$, $La_{1-x}Nd_xFeAsO_{0.65}$, $La_{1-x}Pm_xFeAsO_{0.65}$, $La_{1-x}Sm_xFeAsO_{0.65}$, $La_{1-x}Eu_xFeAsO_{0.65}$, $La_{1-x}Gd_xFeAsO_{0.65}$, $La_{1-x}Tb_xFeAsO_{0.65}$, $La_{1-x}Dy_xFeAsO_{0.65}$, $La_{1-x}Ho_xFeAsO_{0.80}$, $La_{1-x}Er_xFeAsO_{0.75}$, $La_{1-x}Y_xFeAsO_{0.80}$, $La_{1-x}Y_xFeAsO_{0.60}$, $La_{1-x}Sm_xFeAsO_{0.85}$, whose components are isostructural with ZrCuSiAs. It is shown that the magnitude of the mixing energy is determined mainly by the difference in sizes of the substituting structural units. The presented diagram makes it possible to predict the regions of thermodynamic stability of solid solutions, as well as the substitution limits (x) depending on the decomposition temperature (T_d) or the decomposition temperature according to the given substitution limits for limited series of solid solutions in all the above systems. Within the error of the method, our results do not contradict the available experimental data for $La_{1-x}Y_xFeAsO_{0.6}$ and $La_{1-x}Sm_xFeAsO_{0.85}$ systems and can be useful in choosing the ratio of components in «mixed» matrices, as well as the amount of an activator in high-temperature superconductors and effective magnetic materials.

✉ Dr. Serhii Radio
radio@donnu.edu.ua

[1] Vasyl' Stus Donetsk National University, 600-richchia vul. 21, 21021 Vinnytsia, Ukraine
[2] Université d'Angers, rue de Rennes 40 - BP 73532, 49035 Angers cedex 01, France
[3] Minnesota State University, Ford Hall 241, 56001 Mankato, Minnesota, USA

2.1 Introduction: Iron-based layered superconductors

Iron-based layered superconductors ($LnFePnO_{1-y}$, Ln – lanthanides, Pn – P or As) are Fe–containing compounds with a ZrCuSiAs-type of structure (tetragonal, *P*4/*nmm*) whose superconducting properties were discovered in 2006 for LaOFeP [2.1], and in 2008 for fluorine-doped LaFeAsO [2.2].

The structure, depicted in Fig. 2.1, consists of alternating Fe–As and La–O layers. Fe and O atoms sit at the center of slightly distorted As and La tetrahedra; the As tetrahedra are squeezed in the *z* direction. Since the radius of As atoms is much larger than the radius of a Fe atom, the Fe–As blocks are not atomically planar, in contrast to the Cu–O planes of cuprates. Fe atoms form a planar square lattice, with As atoms located above and below this plane, forming tetrahedra with Fe atoms in the center; the Fe–As distance is 2.41 Å, and the As–Fe–As angles are either 107.5^0 or 113.5^0. Fe atoms also bond to other Fe atoms in the plane, which are arranged on a square lattice at a distance of 2.85 Å [2.2–2.3]. Crystallochemical properties of LnFeAsO compounds are determined by the configuration of the outer electron shells: Fe(4s4p3d), As(4s4p), Ln(6s5d4f), O(2s2p). The formal valences of ions are as follows: La^{3+}, O^{2-}, Fe^{2+}, and As^{3-}. It is thought that these two layers are, respectively, positively and negatively charged, and that the La–O chemical bond in the La–O layer is ionic whereas the Fe–As has a predominantly covalent nature. Thus, the chemical formula may be expressed as $(La^{3+}O^{2-})^{+}(Fe^{2+}As^{3-})^{-}$. The conductive carriers, the concentration of which can be increased by substitution of the O^{2-} ion with a F^{-} ion, are confined two dimensionally in the $(FeAs)^{-}$ layers (Fig. 2.1) [2.4].

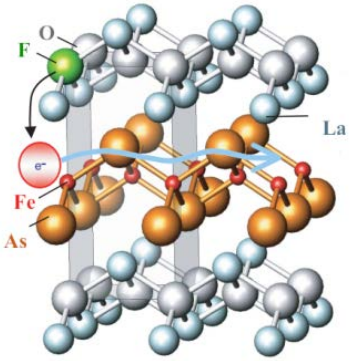

Fig. 2.1 – Crystal structure of LaFeAsO1–xFx. Adapted from Ref. [2.4]

Crystal lattice parameters and superconducting transition temperatures for some compounds LnFeAsO are given in Table 2.1.

Table 2.1. Maximal temperatures of superconducting transitions obtained by doping of LnFeAsO compounds.

$LnFeAsO_{1-y}F_y$ or $LnFeAsO_y$	***T*c, K**	***a*, Å**	***c*, Å**
$LaFeAsO_{0.95}F_{0.05}$ [2.2]	26	4.0320	8.7263
LaFeAsO [2.2]		4.0355	8.7393
$LaFeAsO_{0.89}F_{0.11}$ [2.4]	43 (at 4 GPa) 9 (at 30 GPa)	–	–
$LaFeAsO_{0.8}F_{0.2}$ [2.5]	27.5±0.2	4.030	8.716
LaFeAsO [2.5]		4.039	8.742
$LaFeAsO_{0.85}$ [2.6]	31.2	4.022	8.707
LaFeAsO [2.6]		4.033	8.739
$CeFeAsO_{0.84}F_{0.16}$ [2.7]	41	3.989	8.631
CeFeAsO [2.7]		3.996	8.648
$CeFeAsO_{0.88}F_{0.12}$ [2.8]	47 (at 1.8 GPa) 4.5 (at 19 GPa) <1.1 (at 26.5 GPa)	–	–
$CeFeAsO_{0.85}$ [2.6]	46.5	3.979	8.605
CeFeAsO [2.6]		3.998	8.652
$PrFeAsO_{0.89}F_{0.11}$ [2.9]	52	3.967	8.561
PrFeAsO [2.9]		3.9853 (y = 0)	8.595
$PrFeAsO_{0.85}$ [2.6]	51.3	3.968	8.566
PrFeAsO [2.6]		3.985	8.600
$NdFeAsO_{0.89}F_{0.11}$ [2.10]	52	–	–
$NdFeAsO_{0.82}F_{0.18}$ [2.11]	50	–	–
$NdFeAsO_{0.85}$ [2.6]	53.5	3.943	8.521
NdFeAsO [2.6]		3.965	8.572
$NdFeAsO_{0.7}F_{0.3}$ [2.12]	46	–	–
$SmFeAsO_{0.90}F_{0.10}$ [2.13]	55	3.915	8.428
SmFeAsO [2.13]		3.933	8.495
$SmFeAsO_{0.85}F_{0.15}$ [2.14]	43	3.932	8.490
SmFeAsO [2.14]		3.940	8.501
$SmFeAsO_{0.85}$ [2.6]	55	3.897	8.407
SmFeAsO [2.6]		3.933	8.795
$GdFeAsO_{0.85}$ [2.15]	53.5	3.890	8.383
GdFeAsO [2.15]		3.903	8.453
$GdFeAsO_{0.8}F_{0.2}$ [2.15]	51.2	–	–
$GdFeAsO_{0.83}F_{0.17}$ [2.16]	36.6	4.001	8.650
$TbFeAsO_{0.85}$ [2.17]	42	3.889	8.376
$TbFeAsO_{0.9}F_{0.1}$ [2.18]	45.5	3.8634	8.333
TbFeAsO [2.18]		3.8632	8.322
$TbFeAsO_{0.8}F_{0.2}$ [2.18]	45.2	3.860	8.332
$TbFeAsO_{1-\delta}$ [2.19]	48.5	3.878	8.354
TbFeAsO [2.19]		3.898	8.404
$DyFeAsO_{0.9}F_{0.1}$ [2.18]	45.3	3.8425	8.2837
$DyFeAsO_{0.8}F_{0.2}$ [2.18]	43.0	3.8530	8.299
$DyFeAsO_{1-\delta}$ [2.19]	52.2	3.859	8.341
$HoFeAsO_{1-\delta}$ [2.19]	50.3	3.846	8.295
$ErFeAsO_{0.75}$ [2.20][a]	35.9	3.8198	8.2517
$ErFeAsO_{0.95}$ [2.20][a]	43.0	3.8238	8.2680
$ErFeAsO_{0.95}$ [2.20][a]	44.5	3.8219	8.2807
$YFeAsO_{1-\delta}$ [2.19]	46.5	3.842	8.303

[a] Nominal starting compositions; polycrystalline samples were synthesized by heating pellets with nominal compositions of $ErFeAsO_{1-y}$ ($1-y = 0.75–0.95$) sandwiched between pellets of $LaFeAsO_{0.8}H_{0.8}$ compositions at 1373 K under pressures of 5.5, 5.0 and 5.0 GPa, respectively [2.20].

Information on the influence of the synthesis time and synthesis temperature on the final temperature of the transition into the superconducting state is very limited in the literature. For the $HoFeAsO_{1-x}F_x$ system, such data was discussed in Ref. [2.21] (see Table 2.2).

Table 2.2. Synthesis conditions (all samples were synthesized at 10 GPa), refined lattice parameters (*a*, *c*) and volume (*V*), T_c, mass fractions, and superconducting volume fractions for $HoFeAsO_{1-x}F_x$ samples [2.21].

Sample	t_{synth}, hr	T_{synth}, °C	*a*, Å	*c*, Å	*V*, Å^3	T_c, K	Mass frac., %	Diamag. frac., %
1	2	1 150	3.8246	8.254	120.74	29.3	75	70
2	2	1 100	3.8272	8.2649	121.06	33.0	74	85
3	1	1 150	3.8258	8.264	120.96	33.2	73	76
4	3	1 100	3.8282	8.261	121.07	33.7	84	74
5	2	1 100	3.8282	8.2654	121.13	35.2	81	57
6	2	1 100	3.8297	8.270	121.30	36.2	58	46

Although all samples in Table 2.2 have the same starting composition, small variations in synthesis pressure and temperature result in a dispersion in *x* around the nominal 0.1 value for the $HoFeAsO_{1-x}F_x$ phase and corresponding variations in superconducting properties. T_c increases to a maximum value, T_c(max), at the upper solubility limit of *x* in $LnFeAsO_{1-x}F_x$ systems [2.14], and this is consistent with the observation that the superconducting phases in samples 1, 3, and 4, which are heated at high temperatures or for longer times and so are likely to have a slightly lower F content, have lower T_c (an average value of 32.1 K) compared to other three samples with the average value T_c = 34.8 K, made under nominally identical "optimum" conditions. Sample 6 shows the highest T_c = 36.2 K and the lowest proportion of the diamagnetic fraction in the $HoFeAsO_{1-x}F_x$ phase. This demonstrates that the sample is at the upper limit of the superconducting composition range and so gives a realistic T_c(max) for the $HoFeAsO_{1-x}F_x$ system [2.21].

Also of interest are systematic studies of the pressure effect on properties of the obtained materials. In Ref. [2.22], single-phase polycrystalline samples of oxygen-deficient oxypnictide superconductors $LnFeAsO_{0.7}$ (Ln = Sm, Gd, Tb, and Dy) were synthesized using high-pressure technique. It was found out that the synthesis pressure is a key parameter for synthesizing samples, in particular, for heavier lanthanides. It was established that the lattice parameters systematically decrease with the atomic number of Ln, reflecting the

shrinkage of Ln ionic radius: for the lighter Ln atoms (La, Ce, Pr, Nd), T_c increases monotonously with decreasing the lattice parameters from 26 K for La to 54 K for Nd, then stays at the constant value around 53 K in the case of the heavier lanthanides (Nd, Sm, Gd, Tb, and Dy) (see Fig. 2.2). Obtained results suggest the intimate relationship between the crystal structural parameters and superconductivity, as well as the possible existence of the inherent maximum of T_c located around 50 K in the LnFeAsO based materials [2.22].

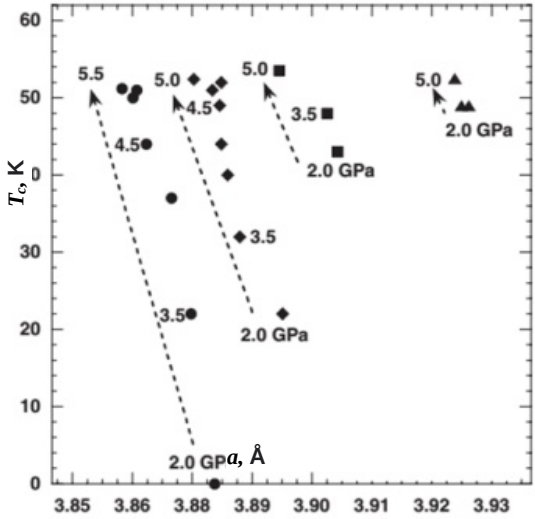

Fig. 2.2 – Relationships between T_c and *a*-axis lattice parameter for the samples with a nominal composition of $LnFeAsO_{0.7}$ (Ln = Sm(▲), Gd(■), Tb(♦), and Dy(●)) synthesized under various pressures ranging from 2.0 to 5.5 GPa. Adapted from Ref. [2.22]

Despite the great interest in high-temperature superconductors based on $LnFeAsO_{1-y}F_y$ and $LnFeAsO_y$ expressed in recent reviews [2.23–2.30] and monographs [2.31–2.33], the data on isomorphous substitutions of lanthanides in Ln positions in the $LnFeAsO_{1-y}$ structure are rather scarce.

The effect of replacing La atoms by Y atoms in the oxypnictide superconductor $LaFeAsO_{0.6}$ was studied in Ref. [2.34]. It has been found that the replacement of La^{3+} by smaller Y^{3+} in the $La_{1-x}Y_xFeAsO_{0.6}$ form leads to the decrease in lattice parameters, and superconducting transition temperature increases monotonically with increasing x up to 43.1 K at $x = 0.5$. Similar

results were obtained in the study of partial substitution of La for Y in the $La_{1-x}Y_xFeAsO_{0.85}F_{0.15}$ superconductor [2.35] that, up to $x = 0.70$, leads to the decrease in lattice parameters a and c of the structure by 1.8 % and 1.7 %, respectively. It was determined that 15 % F-doped samples reach a maximum critical temperature of 40.2 K for the 50 % yttrium substitution. In addition, in the mixed lanthanide compounds of $La_{1-x}Sm_xFeAsO_{0.85}$, the onset superconducting critical temperature was found to rise monotonically from 31.2 K to 55 K with increasing amount of Sm doping from $x = 0$ to 1 [2.36].

Using resistivity and magnetization studies the pressure effect on the superconducting transition temperature of Yb doped $Ce_{0.6}Yb_{0.4}FeAsO_{0.9}F_{0.1}$ has been investigated [2.37]. It has been established that increase in chemical pressure by substitution of smaller Yb^{3+} ions in place of Ce^{3+} ions results in a significant enhancement of T_C from 38 K (Yb free) to 47 K (40 % Yb), enhancement in T_C with external pressure has been observed for this compound up to a maximum value of $T_c = 48.7$ K at 1 GPa, beyond which T_c starts decreasing monotonously.

It is also of interest to study the replacement of three-charged lanthanide cations by ions with a larger charge that can lead to the creation of novel materials with a higher T_c. First studies in this direction showed encouraging results for $Tb_{0.8}Th_{0.2}OFeAs$ [2.38], $Gd_{0.8}Th_{0.2}OFeAs$ [2.39], and $Sm_{0.7}Th_{0.3}OFeAs$ [2.40] where values of $T_c = 52–56$ K were achieved.

2.2 Isomorphous substitutions in the LnFeAsO structure

Isomorphous substitutions of atoms in crystals attract the attention of researchers for the reason that many new inorganic materials (phosphors, semiconductors, ferroelectric, piezoelectrics, etc.) are created on the basis of not individual compounds, but solid solutions. This is due to the fact that the properties in the region of homogeneity regularly change depending on the composition. The properties of high-temperature superconductors (HTSCs) of the first generation based on barium cuprates and rare-earth elements (REEs) are the most studied, both in the case of individual compounds, for example [2.41–2.43], and solid solutions based on them when modified with other REEs [2.44–2.45]. At the same time, REE intersubstitutions for HTSCs with

a tetragonal structure of the ZrCuSiAs type, for which more than 150 representatives are known [2.46–2.47], have been hardly studied.

It is known that undoped LnFeAsO compounds are not superconductors [2.46]. However, those obtained at high pressures (from 2.0 to 5.5 GPa) with a lack of oxygen or with partial substitution of oxygen by fluorine do superconduct [2.34, 2.48]. Isomorphous substitution of lanthanum or iron cations with other cations can lead to an increase in the critical temperature [2.19, 2.48]. Therefore, the study of isomorphous substitutions in superconducting solid solutions is of current interest, as it has been argued in the first chapter above.

To the best of our knowledge, LnFeAsO-based solid solutions with partial REE substitution are described only for a limited number of systems: $La_{1-x}Y_xFeAsO_{0.6}$ (x = 0.0–0.5) [2.34], $La_{1-x}Sm_xFeAsO$ [2.47], and also for $Sm_{1-x/3}Sc_{x/3}FeAsO_{1-x}F_x$ (x = 0.09–0.27) [2.48]. $La_{1-x}Y_xFeAsO_{0.6}$ samples were synthesized by heating LaAs, YAs, Fe, and Fe_2O_3 at 1423 K for 2 h under the pressure of 2 GPa [2.34]. When x changes in the range from 0.0 to 0.4, the unit cell parameters in the $La_{1-x}Y_xFeAsO_{0.6}$ structure naturally decrease from a = 4.029 Å and c = 8.729 Å to a = 3.992 Å and c = 8.652 Å, correspondingly. In this case, the critical temperatures of the superconducting transition increase substantially. However, the experimental determination of substitution limits in this work is not entirely unambiguous. The cell parameters really change in the range of initial compositions x from 0.0 to 0.4, however, only samples with x from 0.0 to 0.1 are single-phase. Samples of initial compositions x from 0.2 to 0.5 consist of several phases that is explained by the fact that the compound of composition YFeAsO does not exist [2.34]. In this case, the $La_{1-x}Y_xFeAsO_{0.6}$ system should be considered multicomponent rather than pseudobinary, and the cell parameters can change in the mixed-phase region. The authors [2.34] believe that the designations they use for the compositions simply mean the nominal value and do not necessarily agree with the actual ones. However, there is another point of view: in Ref. [10] the YFeAsO compound is described and even the cell parameters are given. It is possible that equilibrium was not reached in Ref. [8] due to the fact that the interaction of the components was not completed, since the synthesis was carried out for only 2 h, or partial decomposition of the solid solution occurred when the samples were cooled after calcination.

Similarly, in the $Sm_{1-x/3}Sc_{x/3}FeAsO_{1-x}F_x$ system, as x changes in the range from 0.09 to 0.27, the unit cell parameters also regularly decrease, and the critical superconducting temperatures increase significantly [2.48]. At the same time, samples with $x \geq 0.12$ are also not single-phase, and the authors suggest that $x = 0.23$ is the substitution limit. Apparently, the substitution limit is approximate in this case as well. An increase in the critical temperature T_c can be promoted not only by the substitution of samarium for scandium but also by the substitution of oxygen for fluorine with an ionic radius smaller than that of oxygen.

In Ref. [2.36], the $La_{1-x}Sm_xFeAsO_{0.85}$ system with x = 0, 0.1, 0.2, 0.3, 0.4, 0.6, 0.8, 0.9, 0.95 and 1.0 was synthesized at a final temperature of 1623 K for 2 h. Based on the phase composition and the change in cell parameters, an unlimited substitution of lanthanum for samarium was established in the x range from 0 to 1. In Ref. [2.47], for the same system, it was found that the values of the Ln—O and Ln—As interatomic distances also regularly decrease with increasing x in the entire range of compositions indicating the substitution of lanthanum by samarium. An increase in the transition temperature T_c is due to the compression of the crystal structure, which, in the case of isomorphous substitution by a smaller ion, is even called the «effect of chemical pressure» [2.47].

It should be also noted that the limits of isomorphous substitutions in solid solutions are significantly affected not only by the synthesis temperature but also by pressure. The data on the pressure effect on the critical decomposition (stability) temperature of solid solutions indicate that the pressure growth by 1 GPa leads to its increase by 20–150 degrees [2.49–2.50]. Also, the degree of the pressure influence on the miscibility of the system components depends on the temperature. Studies of solid solutions in the enstatite $Mg_2Si_2O_6$ – diopside $CaMgSi_2O_6$ system carried out at pressures of 5–40 kbar (0.5–4 GPa) and temperatures of 1173–1773 K showed that increasing pressure reduces the mutual miscibility only starting from 1473 K, while at 1173 K the effect of pressure is still very small. The same conclusion follows from the study of the solubility of calcium in olivines at different temperatures and pressures [2.49].

At present, one of the ways to search for HTSCs with desired properties is to study their dependence on the composition in the regions of the solid-

solution existence. At the same time, the physicochemical foundations of the synthesis of solid solutions, such as state diagrams and solubility regions of the $La_{1-x}Ln_xFeAsO_{1-y}$ systems, to the best of our knowledge, are almost not studied. Therefore, in particular, authors studying superconductors based on $LnFeAsO_{1-y}$ in most cases limit themselves by the properties of individual compounds rather than solid solutions.

At the same time, it is known [2.49–2.50] that solid solutions which are synthesized at high temperatures tend to decompose upon cooling that can lead to degradation of materials based on them, changes and irreproducibility of their properties. In this regard, before the synthesis of solid solutions and the study of their properties depending on the composition, it is desirable to know the limits of isomorphous substitutions depending on temperature and stability of solid solutions in the corresponding areas of the systems under synthesis, storage and intended operation conditions. Experimental determination of substitution limits with X-ray diffraction analysis (XRD) by annealing and hardening is complicated by the difficulty of achieving equilibrium at low temperatures due to the low diffusion rate in the solid phase and the possibility of partial decomposition of the solid solution during its quenching from high temperatures. In addition, XRD can be inefficient, in particular, for isostructural components with similar sizes of substituting structural units, in the cases of spinodal decomposition of a solid solution [2.49–2.50] or nanosized particles. In such cases, difficulties arise in determining the substitution limits by XRD, as was the case in the $La_{1-x}Y_xFeAsO_{0.6}$ [2.34] and $Sm_{1-x/3}Sc_{x/3}FeAsO_{1-x}F_x$ systems [2.48].

Insufficient information about substitution limits and stability regions of solid solutions forces researchers to choose the composition of matrices and modifying additives (dopants) either by analogy with related systems or by the «trial and error» method that can lead to excessive consumption of expensive reagents and an increase in the duration of reearch. Thus, for determining the substitution limits, it is rational to use not only experimental but also calculation methods, devoid of the above disadvantages. The aim of our work has been to predict the substitution limits and thermodynamic stability of solid solutions with a structure of the ZrCuSiAs type in a wide range of compositions and temperatures in $La_{1-x}Ln_xFeAsO_{1-y}$ systems with Ln = Ce–Er, and Y.

The choice of such systems was also due to the fact that $LnFeAsO_{1-y}$ superconductors are perspective naterials for generating very strong magnetic fields [2.51].

2.3 Calculation method and initial data

In the general case, according to V. S. Urusov, the mixing energy (interaction parameter) Q which determines possibility and substitution limits, consists of three contributions due to the difference in the sizes of the substituting structural units, the degrees of ionicity of the chemical bond in the components, and the crystal structures of the components [2.49–2.50].

Since we are dealing with the intersubstitution of REE in groups of systems, both components of which are isostructural to ZrCuSiAs, the third contribution is equal to zero. The second contribution, according to [2.49–2.50], must be taken into account in cases where the electronegativity difference $\Delta\chi(Ln^{3+})$ of ions replacing each other is greater than 0.4. Since the value of this difference calculated by us does not exceed 0.111 (Table 1), the mixing energy is calculated using the formula [2.49–2.50]:

$$Q = 1000Cmnz_m z_x \delta^2 \text{ J/mol}, \quad (2.1)$$

where C is an empirical parameter calculated from the expression $C = 20(2\Delta\chi + 1)$ kJ [2.50] by the difference in the electronegativity of the cation and anion, taken from Ref. [2.52]. The electronegativity of the anion $\chi(AsO_{1-y})$ is estimated as the average of the electronegativity of arsenic and oxygen; $n = 6.8$ is the effective coordination number of the substituted structural unit for the $LnFeAsO_{1-y}$ structure calculated according to S. Batsanov [2.53], since in $LnFeAsO_{1-y}$ the REE cation is surrounded by four arsenic anions and four oxide anions located at two significantly different distances (for example, in the $SmFe_{0.92}Co_{0.08}AsO$ structure they are equal to 3.277 and 2,2884 Å, respectively) [2.54]; m is the number of different structural units in the components calculated taking into account the peculiarities of the $LnFeAsO_{1-y}$, layered structure with alternating LnO^+ and $FeAs^-$ layers [2.46]. Since the substitution occurs only in the LnO^+ layers (the Ln—O and Ln—As distances decrease, while the Fe—As distances are constant [2.47]), iron cations are passive in isomorphous substitution and, therefore, in accordance

with Ref. [2.49] were not taken into account in the calculations: $m = 1 + 1 + (1 - y)$ (Table 2); z_m, z_x are moduli of charges of structural units, $z_m = 3$, $z_x = 2{,}5$ are average charges of oxygen and arsenic ions; δ is the relative difference in the sizes of substituting structural units (a size parameter) that was calculated taking into account the assisting rule [2.49] by crystalline ionic radii:

$$\delta = [(r(La^{3+}) - r(Ln^{3+})]/[r(Ln^{3+}) + r(O^{2-})]. \quad (2.2)$$

Crystalline ionic radii of REE were taken according to R. Shannon [2.55] for a coordination number of 7 closest to the effective coordination number of 6.8 according to S. Batsanov [2.53]. The Ln—O distances were taken equal to the sum of the crystalline ionic radii of the cations and the oxide anion: $r(Ln^{3+}) + r(O^{2-})$. The choice of the oxide anion as the common structural unit in calculating δ is due to the fact that it is located in the LnO^+ layer, in which substitution occurs. The crystalline ionic radius of oxygen was taken according to R. Shannon for a coordination number of 4. The accuracy of the calculation of the mixing energy according to the data [2.49] is ± 13 %.

Since the values of the dimensional parameters δ are less than 0.067 (Table 2), according to the recommendations [2.49–2.50], the critical decomposition temperatures of solid solutions were calculated in the approximation of regular solutions by the expression $T_{cr} = Q/2kN$, where k is the Boltzmann constant and N is the Avogadro number. The equilibrium decomposition temperature T_d was calculated from the given substitution limit x or the substitution limit x from the decomposition temperature, according to the Becker equation [2.56]:

$$-(1 - 2x) / \ln[x/(1 - x)] = kN \times T_d/Q. \quad (2.3)$$

In the two cases, the Q value was taken in cal/mol [2.49–2.50].

2.4 Results and discussion

Some initial data and results of calculations of the mixing energy and critical decomposition temperatures T_{cr} are summarized in Tables 2.3–2.4.

Table 2.3. Values of electronegativity of cations $\chi(Ln^{3+})$, the average electronegativity of anions χ(As, O) and constants C calculated for $La_{1-x}Ln_xFeAsO_{1-y}$ solid solutions (Ln = Ce–Er, and Y)

Ln	1–y	$\chi(Ln^{3+})$	$\Delta\chi(Ln^{3+})$	χ(As,O)	χ(As,O) – $\chi(Ln^{3+})$	C, kJ
La	0.65	1.327	–	2.300	0.973	58.92
Ce	0.65	1.348	0.021	2.300	0.952	58.08
Pr	0.65	1.374	0.047	2.300	0.926	57.04
Nd	0.65	1.382	0.055	2.300	0.918	56.72
Pm	0.65	1.391	0.064	2.300	0.909	56.36
Sm	0.65	1.410	0.083	2.300	0.890	55.6
Eu	0.65	1.433	0.106	2.300	0.867	54.68
Gd	0.65	1.386	0.059	2.300	0.914	56.56
Tb	0.65	1.410	0.083	2.300	0.890	55.6
Dy	0.65	1.426	0.099	2.300	0.874	54.96
Ho	0.80	1.433	0.106	2.583	1.150	66.00
Er	0.95	1.438	0.111	2.865	1.427	77.08
Er	0.75	1.438	0.111	2.488	1.051	62.04
Y	0.80	1.340	0.013	2.583	1.150	66.00
Y	0.60	1.340	0.013	2.207	0.867	54.68
Sm	0.85	1.410	0.083	2.677	1.267	70.68

Table 2.4. Some initial data and results of calculation of mixing energies and critical decomposition temperatures for $La_{1-x}Ln_xFeAsO_{1-y}$ solid solutions (Ln = Ce–Er, and Y)

Ln	1–y	$r(Ln^{3+})$, Å	Ln–O, Å	δ	C, kJ	m	Q, J/mol	T_{cr}, K
La	0.65	1.240	2.480		58.92	2.65		
Ce	0.65	1.210	2.450	0.01224	58.08	2.65	1175	70
Pr	0.65	1.198	2.436	0.01806	57.04	2.65	2513	150
Nd	0.65	1.186	2.426	0.02225	56.72	2.65	3794	226
Pm	0.65	1.172	2.412	0.02819	56.36	2.65	6053	361
Sm	0.65	1.160	2.400	0.03333	55.60	2.65	8346	498
Eu	0.65	1.150	2.390	0.03765	54.68	2.65	10474	625
Gd	0.65	1.140	2.380	0.04202	56.56	2.65	13496	806
Tb	0.65	1.120	2.360	0.05084	55.60	2.65	19422	1159
Dy	0.65	1.110	2.350	0.05531	54.96	2.65	22722	1352
Ho	0.80	1.098	2.338	0.06073	66.00	2.80	34759	2075
Y	0.80	1.100	2.340	0.05982	66.00	2.80	33725	2014
Y	0.60	1.100	2.340	0.05982	54.68	2.60	25945	1549
Sm	0.85	1.160	2.400	0.03333	70.68	2.85	11412	681
Er	0.95	1.085	2.325	0.06666	77.08	2.95	51530	3077
Er	0.75	1.085	2.325	0.06666	62.04	2.75	38663	2309

The calculations were carried out for substitutions in the previously oxygen-deficient compounds [2.19, 2.20, 2.22], synthesized by the following procedures:

1. Samples of the $LnFeAsO_{0.8}$ initial composition with Ln = Ho and Y sintered for 1 h at a temperature of 1 273 K and a pressure of 5 GPa. After

turning off the power, the samples were quickly quenched to room temperature by cooling in water for about 1 min and then the pressure was released [2.19].

2. Samples of the $LnFeAsO_{1-y}$ composition (y = 0,60–0,70), synthesized at a pressure of 2.0 GPa for Ln = La, Ce, Pr, Nd, at a pressure of 5.0 GPa for Ln = Sm, Gd, Tb and at a pressure of 5.5 GPa for Ln = Dy. The pellets were heated for 2 h at a synthesis temperature of 1 323–1 373 K for Ln = Gd, Tb, Dy and 1 373–1 423 K for Ln = La, Ce, Pr, Nd and Sm [2.22].

3. Samples with the $ErFeAsO_{1-y}$ nominal composition were synthesized by heating pellets, sandwiched between $LaFeAsO_{0.8}H_{0.8}$ granules at 1 373 K under a pressure of 5.0–5.5 GPa [2.20].

As can be seen from the data presented, with an increase in the atomic number of REEs, values of the dimensional parameter δ, mixing energies Q, and critical decomposition temperatures T_{cr} increase in the series of the $La_{1-x}Ln_xFeAsO_{1-y}$ systems, where Ln = Ce–Er. This is so since in such series of systems the difference between the radii of lanthanum and REE ions increases. According to the calculated values of the critical decomposition temperatures (for x = 0.50) and decomposition temperatures of limited solid solutions (for x = 0.01, x = 0.03, x = 0.05, x = 0.09, see Table 2.5) their dependence on REE numbers for the $La_{1-x}Ln_xFeAsO_{0.65}$ systems with Ln = Ce–Dy (diagram of thermodynamic stability of solid solutions) was plotted in Fig. 2.3.

Table 2.5. Decomposition temperatures (K) of $La_{1-x}Ln_xFeAsO_{0.65}$ solid solutions, where Ln = Ce–Dy, for x = 0.01, 0.03, 0.05, 0.09, and 0.50

x	Ce	Pr	Nd	Pm	Sm	Eu	Gd	Tb	Dy
0,01	30	64	97	154	213	267	344	495	579
0,03	38	81	122	196	269	338	436	627	734
0,05	43	92	138	221	305	382	493	709	830
0,09	50	106	161	256	353	443	571	822	962
0,50	70	150	226	361	498	625	806	1159	1352

The thermodynamic stability diagram was calculated only for $La_{1-x}Ln_xFeAsO_{0.65}$ systems, where Ln = Ce–Dy, since the chemical composition of their components in terms of oxygen content is identical and the value $(1-y)$ according to Ref. [2.22] differed only within 0.60–0.70 (for the calculations, an average value of 0.65 was taken).

It follows from the presented diagram that the continuous series of solid solutions for the $La_{1-x}Ln_xFeAsO_{0.65}$ systems (Ln = Ce–Dy) are thermodynamically stable in the temperature ranges above the critical ones (above curve e).

At lower temperatures (below curve e), they can decompose, forming two series of limited solid solutions in each system, if the diffusion rate is sufficient for the formation and growth of new phases. Similarly, limited solid solutions of limiting compositions $x = 0.01$, $x = 0.03$, $x = 0.05$, and $x = 0.09$ at temperatures in the region above curves a, b, c, and d are thermodynamically stable while below these curves they can decompose. It should be also noted that a change in the oxygen content significantly affects the mixing energy, the critical decomposition temperatures of solid solutions, and, consequently, the stability and substitution limits. Thus, in the $La_{1-x}Ln_xFeAsO_{1-y}$ systems with Ln = Sm, Er, and Y, with growing (1–*y*) values from 0.65, 0.75 and 0.60 to 0.85, 0.95 and 0.80, the critical decomposition temperatures increase from 498, 2 309 and 1 549 K to 681, 3 077 and 2 014 K respectively.

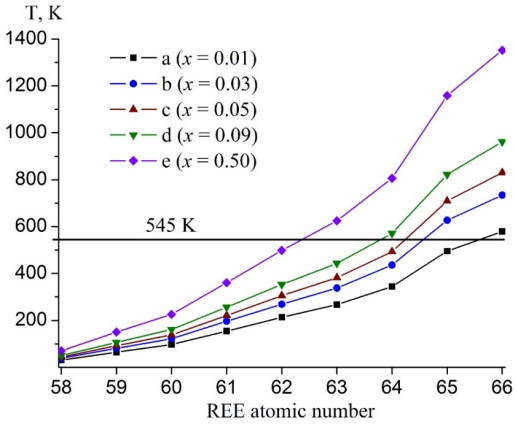

Fig. 2.3 – Diagram of the thermodynamic stability of solid solutions: Dependences of the calculated decomposition temperatures for $La_{1-x}Ln_xFeAsO_{0.65}$ solid solutions (Ln = Ce–Dy) for $x = 0.01$ (a), $x = 0.03$ (b), $x = 0.05$ (c), $x = 0.09$ (d), and $x = 0.50$ (e) of the REE atomic number. Below the horizontal line at 545 K, solid solutions can become metastable

It is known that with decreasing temperature the mobility of the solid-solution structural units reduces due to the diminishing diffusion rate and the solubility regions become narrower [2.49–2.50]. This happens until the diffusion rate becomes so small that the decrease in the solubility regions practically stops, i. e., spontaneous hardening occurs and solid solutions can be metastable. If we assume that the spontaneous hardening temperature is close

to the temperature at which the components begin to interact when their mixture is heated, leading to the formation of a solid solution, we can estimate the spontaneous hardening temperature and the metastability region [2.57]. For example, as was shown in Ref. [2.46], the BiCuSO compound with the ZrCuSiAs structure, similar in composition to LnFeAsO, was synthesized by the low-temperature hydrothermal method at 520 K or using freshly prepared highly reactive precursor compounds at 570 K. Therefore, it can be assumed that spontaneous hardening of solid solutions of the systems under consideration can occur at temperatures of ~545 K and less.

Thus, the $La_{1-x}Ln_xFeAsO_{0.65}$ systems with Ln = Ce–Dy, continuous series of solid solutions, are thermodynamically stable above the critical decomposition temperatures of 70–1 352 K (Table 2.4, Fig. 2.3, curve *e*). With decreasing temperatures, they become thermodynamically unstable and can split into two regions of limited solid solutions. At temperatures below ~545 K solid solutions should not decompose, that is, spontaneous hardening will take place and they will come to be metastable.

Based on the foregoing, it can be assumed that continuous series of solid solutions in the $La_{1-x}Ln_xFeAsO_{0.65}$ systems, where Ln = Ce–Pm, in the range of temperatures above the critical one (above 70, 150, 226, and 361°K, respectively) will be thermodynamically stable, and below critical temperatures do not decompose, i. e., become metastable.

In the range from melting temperatures to critical ones (625, 806, 1 159, 1 352 K respectively), continuous series of solid solutions in the $La_{1-x}Ln_xFeAsO_{0.65}$ systems with Ln = Eu–Dy will be thermodynamically stable. In the temperature range from critical one to ~ 545 K they will decompose into two solid solutions, which will become metastable at lower temperatures. Since the critical temperature of the $La_{1-x}Sm_xFeAsO_{0.65}$ solid solutions (498 K) differs from the spontaneous hardening temperature (~ 545 K) within the calculational error, it is not possible to conclude unequivocally about their behaviour at temperatures close to the critical one.

According to Fig. 2.3, one can visually estimate the decomposition temperature of limited series of solid solutions by setting the substitution limit or determine the substitution limit of lanthanum for REE by setting the decomposition temperature. To find the substitution limit for a given temperature, it

is necessary to draw an isotherm until it intersects with a vertical line drawn from the REE number. This will determine the range of compositions in which there is a substitution limit, and the interpolation of the vertical segment between the two nearest curves gives this substitution limit. The slatter can be determined more precisely by constructing for a specific system the dependence of the decomposition temperatures calculated from the Becker equation on the composition (the dome of decomposition), which, in the approximation of regular solid solutions, will be symmetrical.

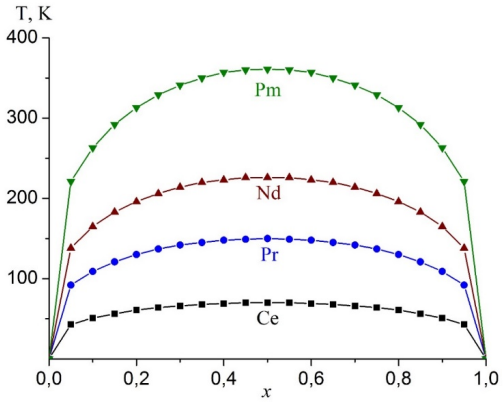

Fig. 2.4 – Calculated domes of the solid solutions decomposition for $La_{1-x}Ln_xFeAsO_{0.65}$ systems

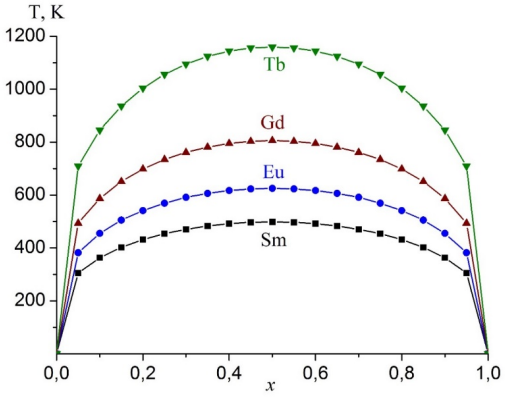

Fig. 2.5 – Calculated domes of the solid solutions decomposition for the $La_{1-x}Ln_xFeAsO_{0.65}$ systems

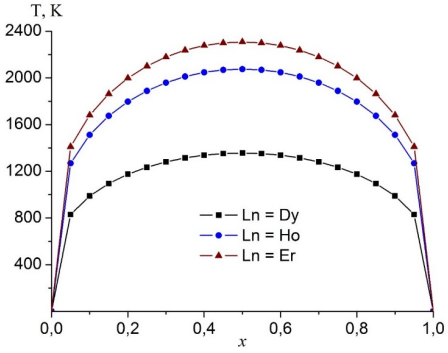

Fig. 2.6 – Calculated domes of the solid solutions decomposition for $La_{1-x}Ln_xFeAsO_{1-y}$ systems with Ln = Dy (1–y = 0.65) (■); Ln = Ho (1–y = 0.80) (●); Ln = Er (1–y = 0.75) (▲)

To do this, using the Becker equation, the decomposition temperatures for the $La_{1-x}Ln_xFeAsO_{1-y}$ systems, where Ln = Ce–Er, and Y, were calculated in the composition range $1{,}0 > x > 0$ with the step $x = 0.05$ and the dependences of the decomposition temperatures on the composition (domes of decomposition, Fig. 2.4–2.8) were plotted. Using them, with greater accuracy, one can graphically determine the equilibrium composition at a given temperature, or the decomposition temperature at a given composition, as well as the stability regions of solid solutions.

2.5 Comparison of calculation results with literature data

To the best of our knowledge, there are no literature data concerning mixing energies and critical decomposition temperatures in the $La_{1-x}Ln_xFeAsO_{1-y}$ systems. This, of course, makes it difficult to assess the reliability of the calculations performed. At the same time, there is information about experimental studies of isomorphous substitutions of lanthanum for yttrium in the $La_{1-x}Y_xFeAsO_{0.6}$ system [2.34] and lanthanum for samarium in the $La_{1-x}Sm_xFeAsO_{0.85}$ system [2.36]. In the $La_{1-x}Y_xFeAsO_{0.6}$ system, the substitution limit of lanthanum for yttrium at 1 423 K was not determined in Ref. [2.34]. Using the XRD method it was shown that the single-phase region extends up to $x = 0.1$ inclusive, the non-single-phase region is located at $x \geq 0.2$, and the cell parameters decrease in the region up to $x = 0.4$. It follows

from this that the substitution limit is in the interval between 0.1 and 0.4, which does not contradict the limit $x = 0.27$ calculated by us (Fig. 2.7) that is in the middle of this interval.

In the $La_{1-x}Sm_xFeAsO_{0,85}$ system, compositions with $x = 0$, 0.1, 0.2, 0.3, 0.4, 0.6, 0.8, 0.9, 0.95, and 1.0 were previously studied [2.36]. According to the phase composition and the change in cell parameters, unlimited substitution of lanthanum for samarium in the x range from 0 to 1 was established. This does not oppose the calculation results, since the established unlimited miscibility of the components [2.36] is in the temperature range above 681 K which is predicted by us for the thermodynamic stability of continuous series of solid solutions, see Table 2.4 and Fig. 2.8.

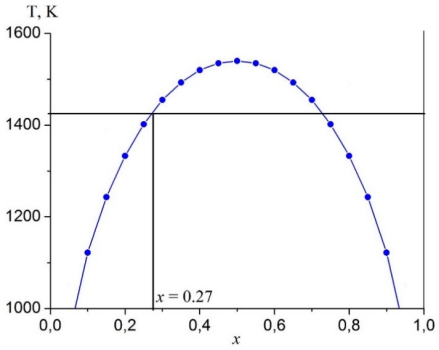

Fig. 2.7 – Calculated dome of the solid solutions decomposition for the $La_{1-x}Y_xFeAsO_{0.6}$ system. The straight line at 1 423 K is the temperature of the solid solution synthesis [2.34]

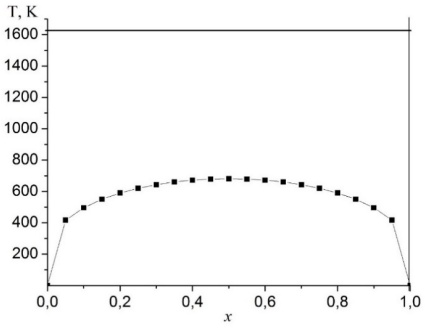

Fig. 2.8 – Calculated dome of the solid solutions decomposition for the La1–xSmxFeAsO0.85 system. The straight line at 1 623 K is the temperature of the solid solution synthesis [2.36]

2.6 Conclusions

1. Within the approximation of regular solid solutions and using the crystal-chemical approach by V. S. Urusov, the mixing energies (interaction parameters) and critical decomposition (stability) temperatures of solid solutions of the $La_{1-x}Ln_xFeAsO_{1-y}$ systems (Ln = Ce–Er, and Y) with the ZrCuSiAs structure have been calculated.

2. With an increase in the REE number, the calculated mixing energies and critical decomposition temperatures for the $La_{1-x}Ln_xFeAsO_{1-y}$ solid solutions grow in the Ce–Er series of the rare earth elements.

3. It is shown that the magnitude of the mixing energy is determined mainly by the difference in sizes of the substituting structural units of the system components.

4. The presented thermodynamic stability diagram for the $La_{1-x}Ln_xFeAsO_{0.65}$ systems with Ln = Ce–Dy makes it possible to visually evaluate not only the thermodynamic stability, instability, and supposed metastability of solid solutions in a wide range of compositions and temperatures, but also the substitution limits for limited series of solid solutions according to a given decomposition temperature, or their decomposition temperature according to a given substitution limit.

5. Continuous series of solid solutions in the $La_{1-x}Ln_xFeAsO_{0.65}$ systems (Ln = Ce–Pm) in the range of temperatures above the critical ones (above 70, 150, 226, 361 K, respectively) will be thermodynamically stable, and below the critical ones they cannot decompose, i. e., become metastable. In the range of temperatures above the critical ones (625, 806, 1 159, 1 352 K, respectively), continuous series of solid solutions in the $La_{1-x}Ln_xFeAsO_{0.65}$ systems with Ln = Eu–Dy will be thermodynamically stable. In the temperature range from critical values to ~ 545 K, they will decompose into two solid solutions, which will become metastable at lower temperatures.

6. The decomposition temperatures of solid solutions in the $La_{1-x}Ln_xFeAsO_{1-y}$ systems, where Ln = Ce–Er and Y, have been calculated in the composition range $1.0 > x > 0$ with the step $x = 0.05$ and the dependences of their decomposition temperatures on the composition (domes of decomposition) were plotted.

7. The calculation results do not contradict experimental data for $La_{1-x}Y_xFeAsO_{0.6}$ and $La_{1-x}Sm_xFeAsO_{0.85}$ systems obtained by other research groups [2.34, 2.36].

2.7 References to chapter 2

2.1 Kamihara Y., Hiramatsu H., Hirano M., Kawamura R., Yanagi H., Kamiya T., Hosono H. Iron-based layered superconductor: LaOFeP. *J. Am. Chem. Soc.* 2006. V. 128. P. 10012–10013.

2.2 Kamihara Y., Watanabe T., Hirano M., Hosono H. Iron-based layered superconductor $La[O_{1-x}F_x]FeAs$ (x = 0.05–0.12) with T_c = 26 K. *J. Am. Chem. Soc.* 2008. V. 130. P. 3296–3297.

2.3 Boeri L., Dolgov O. V., Golubov A. A. Is $LaFeAsO_{1-x}F_x$ an electron-phonon superconductor? *Phys. Rev. Lett.* 2008. V. 101. P. 026403.

2.4 Takahashi H., Igawa K., Arii K., Kamihara Y., Hirano M., Hosono H. Superconductivity at 43 K in an iron-based layered compound $LaO_{1-x}F_xFeAs$. *Nature*. 2008. V. 453. P. 376–378.

2.5 Shekhar Ch., Singh S., Siwach P. K., Singh H. K., Srivastava O. N. Synthesis and microstructural studies of iron oxypnictide $LaO_{1-x}F_xFeAs$ superconductors. *Supercond. Sci. Technol.* 2009. V. 22. P. 015005.

2.6 Ren Zh.-A., Che G.-C., Dong X.-L., Yang J., Lu W., Yi W., Shen X.-L., Li Zh.-C., Sun L.-L., Zhou F., Zhao Zh.-X. Superconductivity and phase diagram in iron-based arsenic-oxides $ReFeAsO_{1-\delta}$ (Re = rare-earth metal) without fluorine doping. *Europhys. Lett.* 2008. V. 83. P. 17002.

2.7 Chen G. F., Li Z., Wu D., Li G., Hu W. Z., Dong J., Zheng P., Luo J. L., Wang N. L. Superconductivity at 41 K and its competition with spin-density-wave instability in layered $CeO_{1-x}F_xFeAs$. *Phys. Rev. Lett.* 2008. V. 100. P. 247002.

2.8 Zocco D. A., Hamlin J. J., Baumbach R. E., Maple M. B., McGuire M. A., Sefat A. S., Sales B. C., Jin R., Mandrus D., Jeffries J. R., Weir S. T., Vohra Y. K. Effect of pressure on the superconducting critical temperature of $La[O_{0.89}F_{0.11}]FeAs$ and $Ce[O_{0.88}F_{0.12}]FeAs$. *Phys. C: Supercond.* 2008. V. 468. P. 2229–2232.

2.9 Ren Z. A., Yang J., Lu W., Yi W., Che G. C., Dong X. L., Sun L. L., Zhao Z. X. Superconductivity at 52 K in iron based F doped layered

quaternary compound $Pr[O_{1-x}F_x]FeAs$. *Mater. Res. Innov.* 2008. V. 12. P. 105–106.

2.10 Ren Z.-A., Yang J., Lu W., Yi W., Shen X.-L., Li Z.-C., Che G.-C., Dong X.-L., Sun L.-L., Zhou F., Zhao Z.-X. Superconductivity in the iron-based F-doped layered quaternary compound $Nd[O_{1-x}F_x]FeAs$. *Europhys. Lett.* 2008. V. 82. P. 57002.

2.11 Cheng P., Yang H., Jia Y., Fang L., Zhu X., Mu G., Wen H.-H. Hall effect and magnetoresistance in single crystals of $NdFeAsO_{1-x}F_x$ (x = 0 and 0.18). *Phys. Rev. B.* 2008. V. 78. P. 134508.

2.12 Jaroszynski J., Hunte F., Balicas L., Jo Y.-J., Raičević I., Gurevich A., Larbalestier D. C., Balakirev F. F., Fang L., Cheng P., Jia Y., Wen H. H. Upper critical fields and thermally-activated transport of $NdFeAsO_{0.7}F_{0.3}$ single crystal. *Phys. Rev. B.* 2008. V. 78. No. 174523.

2.13 Ren Zh.-A., Lu W., Yang J., Yi W., Shen X.-L., Li Zh.-C., Che G.-C., Dong X.-L., Sun L.-L., Zhou F., Zhao Zh.-X. Superconductivity at 55 K in iron-based F-doped layered quaternary compound $Sm[O_{1-x}F_x]FeAs$. *Chin. Phys. Lett*. 2008. V. 25. P. 2215–2216.

2.14 Chen X. H., Wu T., Wu G., Liu R. H., Chen H., Fang D. F. Superconductivity at 43 K in $SmFeAsO_{1-x}F_x$. *Nature*. 2008. V. 453. P. 761–762.

2.15 Yang J., Li Zh.-C., Lu W., Yi W., Shen X.-L., Ren Zh.-A., Che G.-C., Dong X.-L., Sun L.-L., Zhou F., Zhao Zh.-X. Superconductivity at 53.5 K in $GdFeAsO_{1-\delta}$. *Supercond. Sci. Technol.* 2008. V. 21. P. 082001.

2.16 Cheng P., Fang L., Yang H., Zhu X., Mu G., Luo H.-Q., Wang Zh.-Sh., Wen H.-H. Superconductivity at 36 K in gadolinium-arsenide oxides $GdO_{1-x}F_xFeAs$. *Sci. China: Phys. Mech. Astron.* 2008. V. 51. P. 719–722.

2.17 Shi Y. G., Yu S., Belik A. A., Matsushita Y., Tanaka M., Katsuya Y., Kobayashi K., Yamaura K., Takayama-Muromachi E. Synthesis and superconducting properties of the iron oxyarsenide $TbFeAsO_{0.85}$. *J. Phys. Soc. Jpn.* 2008. V. 77. P. 155–157.

2.18 Bos J.-W. G., Penny G. B. S., Rodgers J. A., Sokolov D. A., Huxley A. D., Attfield J. P. High pressure synthesis of late rare earth RFeAs(O,F) superconductors; R = Tb and Dy. *Chem. Commun*. 2008. V. 31. P. 3634–3635.

2.19 Yang J., Shen X.-L., Lu W., Yi W., Li Z.-C., Ren Z.-A., Che G.-C., Dong X.-L., Sun L.-L., Zhou F. Zhao Z.-X. Superconductivity in some

heavy rare-earth iron arsenide $REFeAsO_{1-\delta}$ (RE = Ho, Y, Dy and Tb) compounds. *New J. Phys*. 2009. V. 11. P. 025005.

2.20 Shirage P. M., Miyazawa K., Kihou K., Lee Ch.-H., Kito H., Tokiwa K., Tanaka Y., Eisaki H., Iyo A. Synthesis of ErFeAsO-based superconductors by the hydrogen doping method. *Europhys. Lett.* 2010. V. 92. P. 57011.

2.21 Rodgers J. A., Penny G. B. S., Marcinkova A., Bos J.-W. G., Sokolov D. A., Kusmartseva A., Huxley A. D., Attfield J. P. Suppression of the superconducting transition of $RFeAsO_{1-x}F_x$ (R = Tb, Dy, and Ho). *Phys. Rev. B.* 2009. V. 80. P. 052508.

2.22 Miyazawa K., Kihou K., Shirage P. M., Lee Ch.-H., Kito H., Eisaki H., Iyo A. Superconductivity above 50 K in $LnFeAsO_{1-y}$ (Ln = Nd, Sm, Gd, Tb, and Dy) synthesized by high-pressure technique. *J. Phys. Soc. Jpn.* 2009. V. 78. P. 034712.

2.23 Sadovskii M. V. High-temperature superconductivity in iron-based layered iron compounds. *Phys.-Usp.* 2008. V. 51, P. 1201–1227.

2.24 Ishida K., Nakai Y., Hosono H. To what extent iron-pnictide new superconductors have been clarified: a progress report. *J. Phys. Soc. Jpn*. 2009. V. 78. P. 062001.

2.25 Oh H., Moon J., Shin D., Moon Ch.-Y., Choi H. J. Brief review on iron-based superconductors: are there clues for unconventional superconductivity? *Prog. Supercond. Cryog.* 2011. V. 13. P. 65–84.

2.26 Si Q., Yu R., Abrahams E. High-temperature superconductivity in iron pnictides and chalcogenides. *Nat. Rev. Mater.* 2016. V. 1. P. 16017.

2.27 Hosono H., Yamamoto A., Hiramatsu H., Ma Y. Recent advances in iron-based superconductors toward applications. *Mater. Today*. 2018. V. 21. P. 278–302.

2.28 Rasaki S. A., Thomas T., Yang M. Iron based chalcogenide and pnictide superconductors: From discovery to chemical ways forward. *Prog. Solid. State Ch.* 2020. V. 59. P. 100282.

2.29 Song C., Ma X., Xue Q. Emergent high-temperature superconductivity at interfaces. *MRS Bulletin*. 2020. V. 45. P. 366–372.

2.30 Fernandes R. M., Coldea A. I., Ding H., Fisher I. R., Hirschfeld P. J., Kotliar G. Iron pnictides and chalcogenides: a new paradigm for superconductivity. *Nature*. 2022. V. 601. P. 35–44.

2.31 Izyumov Yu., Kurmaev E. High-T_c superconductors based on FeAs compounds. Springer Series in Materials Science. Vol. 143. Springer Heidelberg Dordrecht London New York. 2010.
2.32 Iron-Based Superconductors. Edited by N.-L. Wang, H. Hosono, P. Dai. Pan Stanford Publishing: Taylor & Francis Group. 2013.
2.33 Mancini F., Citro R. The Iron Pnictide Superconductors: An Introduction and Overview. Springer Series in Solid-State Sciences. Vol. 186. Springer International Publishing AG. 2017.
2.34 Shirage P. M., Miyazawa K., Kito H., Eisaki H., Iyo A. Superconductivity at 43 K at ambient pressure in the iron-based layered compound $La_{1-x}Y_xFeAsO_y$. *Phys. Rev. B.* 2008. V. 78. P. 172503.
2.35 Tropeano M., Fanciulli C., Canepa F., Cimberle M. R., Ferdeghini C., Lamura G., Martinelli A., Putti M., Vignolo M., Palenzona A. Effect of chemical pressure on spin density wave and superconductivity in undoped and 15 % F-doped $La_{1-y}Y_yFeAsO$ compounds. *Phys. Rev. B.* 2009. V. 79. P. 174523.
2.36 Yi W., Yang J., Shen X.-L., Lu W., Li Zh.-C., Ren Zh.-A., Che G.-C., Dong X.-L., Zhou F., Sun L.-L., Zhao Zh.-X. Superconductivity in the mixed rare earth iron oxyarsenide $La_{1-x}Sm_xFeAsO_{0.85}$. *Supercond. Sci. Technol.* 2008. V. 21. P. 125022.
2.37 Arumugam S., Kanagaraj M., Tamil Selvan N. R., Esakki Muthu S., Prakash J., Thakur G. S., Ganguli A. K., Yoshino H., Murata K., Matsubayashi K., Uwatoko Y. Pressure effects on the superconducting transition of ytterbium doped $Ce_{0.6}Yb_{0.4}FeAsO_{0.9}F_{0.1}$. *Phys. Status Solidi RRL*. 2012. V. 6. P. 220–222.
2.38 Li L.-J., Li Y.-K., Ren Z., Luo Y.-K., Lin X., He M., Tao Q., Zhu Zh.-W., Cao G.-H., Xu Zh.-A. Superconductivity above 50 K in $Tb_{1-x}Th_xFeAsO$. *Phys. Rev. B.* 2008. V. 78. P. 132506.
2.39 Wang C., Li L., Chi S., Zhu Z., Ren Z., Li Y., Wang Y., Lin X., Luo Y., Jiang S., Xu X., Cao G., Xu Z. Thorium-doping–induced superconductivity up to 56 K in $Gd_{1-x}Th_xFeAsO$. *Europhys. Lett.* 2008. V. 83. P. 67006.
2.40 Zhigadlo N. D., Katrych S., Weyeneth S., Puzniak R., Moll P. J. W., Bukowski Z., Karpinski J., Keller H., Batlogg B. Th-substituted

SmFeAsO: Structural details and superconductivity with T_C above 50 K. *Phys. Rev. B.* 2010. V. 82. P. 064517.

2.41 Ohmukai M., Fujita T., Ohn T. The Temperature dependence of critical current in $YBa_2Cu_3O_{7-d}$ thin films deposited on MgO by an eclipse PLD. *Braz. J. Phys*. 2001. V. 31. P. 511–513.

2.42 Conradson S. D., Raistrick I. D. The Axial Oxygen Atom and Superconductivity in $YBa_2Cu_3O_7$. *Science*. 1989. V. 243. P. 1340–1343.

2.43 Moriya K., Igarashi K., Watanabe H., Hasegawa H., Sasaki T., Yasuda A. Growth of $YBa_2Cu_3O_7$ superconductor thin films using ethanolamine-based solutions via simple spin coating. *Results. Phys.* 2018. V. 11. P. 364–367.

2.44 Dhami A. K., Basak S., Ghatak S. K., Dey T. K. Thermoelectric power of samarium substituted $Y_{1-x}Sm_xBa_2Cu_3O_{7-\delta}$ superconducting pellets. *Mater. Res. Bull.* 2001. V. 36. P. 971–980.

2.45 Haugan T. J., Campbell T. A., Pierce N. A., Locke M. F., Maartense I., Barnes P. N. Microstructural and superconducting properties of $(Y_{1-x}Eu_x)Ba_2Cu_3O_{7-\delta}$ thin films: x = 0–1. *Supercond. Sci. Technol.* 2008. V. 21. P. 025014.

2.46 Pöttgen R., Johrendt D. Materials with ZrCuSiAs-type structure. *Z. Naturforsch. B.* 2008. V. 63b. P. 1135–1148.

2.47 Iadecola A., Joseph B., Paris E., Provino A., Martinelli A., Manfrinetti P., Putti M., Saini N. L. Effect of chemical pressure on the local structure of $La_{1-x}Sm_xFeAsO$ system. *Supercond. Sci. Technol*. 2015. V. 28. P. 025007.

2.48 Chen H., Zheng M., Fang A., Yang J., Huang F., Xie X., Jiang M. Enhanced superconductivity of SmFeAsO Co-doped by scandium and fluorine to increase chemical inner pressure. *J. Solid State Chem.* 2012. V. 194. P. 59–64.

2.49 Urusov V. S. Teoriia izomorfnoi smesimosti [The Theory of Isomorphous Miscibility]. Moscow: Nauka. 1977. (in Russian).

2.50 Urusov V. S., Tauson B. L., Akimov V. V. Geokhimiya tverdogo tela [Solid state geochemistry]. Moscow: GEOS. 1997. (in Russian).

2.51 Hunte F., Jaroszynski J., Gurevich A., Larbalestier D. C., Jin R., Sefat A. S., McGuire M. A., Sales B. C., Christen D. K., Mandrus D. Two-

band superconductivity in $LaFeAsO_{0.89}F_{0.11}$ at very high magnetic fields. *Nature*. 2008. V. 453. P. 903–905.

2.52 Li K., Xue D. Estimation of electronegativity values of elements in different valence states. *J. Phys. Chem. A.* 2006. V. 110. P. 11332–11337.

2.53 Batsanov S. S. Ob effektivnom koordinatsionnom chisle atomov v kristallakh [On the effective coordination number of atoms in crystals]. *Zh. Neorg. Khim*. 1977. V. 22. P. 1155–1159. (in Russian).

2.54 Zhigadlo N. D., Weyeneth S., Katrych S., Moll P. J. W., Rogacki K., Bosma S., Puzniak R., Karpinski J., Batlogg B. High-pressure flux growth, structural, and superconducting properties of LnFeAsO (Ln = Pr, Nd, Sm) single crystals. *Phys. Rev. B.* 2012. V. 86. P. 214509.

2.55 Shannon R. D. Revised effective ionic radii and systematic studies of interatomic distances in halides and chalcogenides. *Acta Cryst. Sect. A.* 1976. V. A32. P. 751–767.

2.56 Becker R. Über den aufbau binarer legierungen (On the constitution of binary alloys). *Zeit. Metal*. 1937. V. 29. P. 245–249. (in German).

2.57 Get'man E. I., Radio S. V., Ignatova L. B., Ardanova L. I. Energies of mixing (interaction parameters), substitution limits, and phase stability of solid solutions $Lu_{1-x}Ln_xVO_4$ (Ln = Ce–Yb, Sc, Y). *Russ. J. Inorg. Chem*. 2019. V. 64. P. 118–124.